Available online at www.sciencedirect.com
SCIENCE DIRECT®
Journal of Sound and Vibration 284 (2005) 1051–1073
JOURNAL OF SOUND AND VIBRATION
www.elsevier.com/locate/jsvi

Leak location using the pattern of the frequency response diagram in pipelines: a numerical study

Pedro J. Lee[a,*], John P. Vítkovský[a], Martin F. Lambert[a], Angus R. Simpson[a], James A. Liggett[b]

[a]*School of Civil & Environmental Engineering, Centre for Applied Modelling in Water Engineering, The University of Adelaide, Adelaide SA 5005, Australia*
[b]*School of Civil & Environmental Engineering, Cornell University, Ithaca, NY 14853-3501, USA*

Received 20 October 2003; received in revised form 15 June 2004; accepted 26 July 2004
Available online 23 November 2004

Abstract

This paper presents a method of leak detection in a single pipe where the behaviour of the system frequency response diagram (FRD) is used as an indicator of the pipe integrity. The presence of a leak in a pipe imposes a pattern on the resonance peaks of the FRD that can be used as a clear indication of leakage. Analytical expressions describing the pattern of the resonance peaks are derived. Illustrations of how this pattern can be used to individually locate and size multiple leaks within the system are presented. Practical issues with the technique, such as the procedure for frequency response extraction, the impact of measurement position, noise- and frequency-dependent friction are also discussed.

1. Introduction

Fluid transients travel at high speeds in liquid-filled pipes collecting information that indicates the pipe condition in the system, making transients an attractive means of

*Corresponding author. Tel.: +61 8 8303 6003; fax: +61 8 8303 4359.
E-mail addresses: plee@civeng.adelaide.edu.au (P.J. Lee), jvitkovs@civeng.adelaide.edu.au (J.P. Vítkovský), mlambert@civeng.adelaide.edu.au (M.F. Lambert), asimpson@civeng.adelaide.edu.au (A.R. Simpson), jal8@cornell.edu (J.A. Liggett).

0022-460X/$ - see front matter © 2004 Elsevier Ltd. All rights reserved.
doi:10.1016/j.jsv.2004.07.023

Nomenclature

$\|h\|$	magnitude of head perturbation
a	wave speed
A	area of pipeline
A_L	area of leak orifice
C_d	coefficient of discharge for leak orifice
D	diameter of pipeline
f	Darcy–Weisbach friction factor or frequency in the peaks of the FRD
g	gravitational acceleration
h	complex hydraulic grade line perturbation
H	hydraulic grade line elevation or frequency response function
H_L	head at the leak orifice
H_{L0}	steady-state head at the leak
i	imaginary unit, $\sqrt{-1}$
l	length of the uniform pipe section under consideration
L	total length of pipeline
L_1, L_2	lengths of pipe subdivided by the leak
m	peak number
Q	discharge
q	complex discharge perturbation
Q_L	discharge out of the leak orifice
Q_{L0}	steady-state flow out of the leak
Q_{V0}	steady-state flow through the valve
R	frictional resistance term $= (fQ_0)/(gDA^2)$ for turbulent flows or $(64v)/(gAD^2)$ for laminar flows, or Fourier transform of the cross-correlation functions
SF	scaling factor for unsteady friction
t	time
T	transfer function for intact pipe section
U	overall transfer matrix for the pipeline system excluding the oscillating valve
x	distance along pipe
x_L	position of leak measured from upstream boundary
x_L^*	dimensionless position of leak, given by x_L/L
Z	characteristic impedance $= (\mu a^2)/(\mathrm{i}\omega g A)$

Greek letters

ϕ	phase
ε	pipe roughness height
$\Delta\tau$	magnitude of the dimensionless valve aperture perturbation
ΔH_{V0}	steady-state head loss across the valve
μ	propagation constant $= (l/a)\sqrt{-\omega^2 + \mathrm{i}gA\omega R}$
τ	dimensionless valve aperture size
τ_0	mean dimensionless valve aperture size, centre of perturbation
v	kinematic viscosity
ω	frequency
ω_{th}	fundamental frequency of system

determining pipe integrity. A leak in a pipe causes partial reflections of wave fronts that become small pressure discontinuities in the original pressure trace and increase the damping of the overall pressure signal. Such partial reflections act to divert energy away from the main waveform and increase the decay rate of the transient signal. The behaviour of this pressure trace is, therefore, indicative of leaks within the system and can be used as a means of leak detection, e.g. those that use inverse methods to determine parameters in transient models by comparison with observed data (inverse transient analysis [1–4]), transient damping—free-vibrational analysis [5], and also methods that use the time of arrival and magnitude of leak-reflected signals to determine leak location [6–8]. All these published fluid transient leak detection methods share a common theme in that a small amplitude disturbance—a fluid transient—is initiated in a pipe and the subsequent pressure response is measured and analysed to derive system information. This type of

analysis is more commonly known as system response extraction and forms the basis of well-established methodologies used to extract dynamic responses of complex mechanical and electrical systems.

For small transient signals, the impact of nonlinearity in pipeline systems is negligible and, for these cases, the pipeline can be considered as a linear system. The behaviour of such systems is frequency dependent and is commonly summarized in a frequency response diagram (FRD) [9–12]. Whereas resonance frequencies reinforce and transmit input signals, other frequencies are absorbed within the system. In this respect, pipeline systems are similar to frequency filters, the characteristics of which are determined by system properties such as boundary conditions, friction, and wave speed. The FRD describes the degree to which each frequency component in an input signal is amplified or attenuated within the system and can be determined by measurement of the input transient signal and the pressure response from the pipeline. While the type of input transient used for this process is arbitrary, Refs. [13,10] proposed the use of pseudo-random binary sequence (PRBS). PRBS provides an increased signal-to-noise ratio during frequency response extraction and allows the signal to be wide band while staying within the linearity approximations. Further information on PRBS is found in Refs. [13–17], and the extent to which inline valves in the system can be perturbed while staying within the linearity approximation is shown in Ref. [10].

The presence of a leak within a pipe imposes changes on the system response that is observed in the FRD as a pattern on the resonance peaks [11,12]. Lee et al. [11] have shown that the shape of the pattern imposed on the FRD is a function of the leak position, whereas the magnitude of this pattern is related to the size of the leak alone. Ferrante et al. [18] also illustrated the impact of a leak on the FRD and empirical attempts were made to use it as a means of leak detection using the impedance equations. This paper presents an analytical solution that describes the pattern a leak induces on the resonance response for liquid flow in a frictionless pipeline system that can be used to detect, quantify and locate multiple leaks. Issues associated with the possible implementation of this technique, such as the influence of frequency-dependent friction, influence of the measurement position and the limitations of the technique, are also addressed herein.

2. Impact of a leak on the FRD

A leak in a pipe is illustrated in Fig. 1 with the system parameters in Table 1. For simplicity, the simulation results only consider steady friction without the impact of unsteady friction (the impact of unsteady friction will be investigated later in the paper). The transient is generated by the perturbation of an inline valve located at the downstream end of the pipeline. The size of the valve perturbation for the transient generation is kept small to ensure system linearity [10], and the FRD is expressed in terms of measured head variation (in meters) at a point just upstream of the inline valve. The numerical FRD of the intact (no leak) pipe is shown in Fig. 2. From the FRD, the pipeline has equal-magnitude resonance peaks located at odd multiples of the fundamental frequency of the pipe (ω_{th}) and is typical of a system with asymmetrical boundary

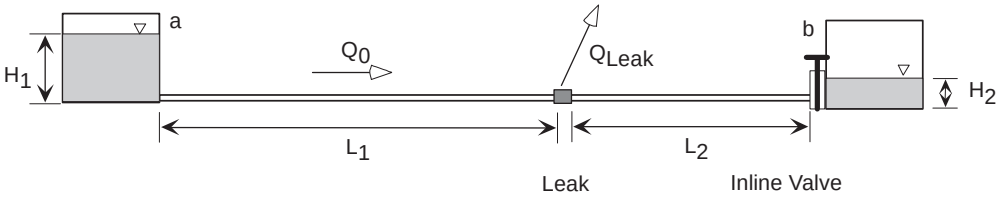

Fig. 1. Single pipeline example for the derivation of the leak-coding equation.

Table 1
System parameters for pipeline example in Fig. 1

Parameter	Value
L_1	1400 m
L_2	600 m
D_1	300 mm
D_2	300 mm
H_1	50.0 m
H_2	20.0 m
A_1	1200 m/s^{-1}
A_2	1200 m/s^{-1}
f_1	0.020
f_2	0.022
$\Delta\tau$	0.1
Q_0	0.0153 m^3 s^{-1}
C_dA_L/A	2×10^{-3}
Leak diameter	15 mm

conditions. The fundamental frequency of the pipeline in radians per second is

$$\omega_{\text{th}} = \frac{\pi a}{2L}, \tag{1}$$

where L and a are the total length and wave speed of the pipe, respectively. Figs. 2 and 3 show the FRD of the single pipe for leaks located at various positions along the pipe and also for varying sizes. The size of a leak is measured in terms of the lumped leak parameter C_dA_L, where C_d is the discharge coefficient of the leak and A_L is the flow area of the leak orifice. The position of the leak is defined in terms of dimensionless leak location x_L^*, and is the distance of the leak from the upstream boundary divided by the total length of the pipeline. The presence of a leak induces a pattern such that the FRD no longer has equal-magnitude peaks. The standard deviation of the peak magnitudes can be used to determine whether a leak exists within the system and, unlike previous leak detection methods, it does not require the comparison to a leak-free case. While the magnitude of the leak affects the magnitude of this pattern (refer to Fig. 3), it is the position of the leak within the pipe that leads to a change in the shape of the FRD. The following section derives this leak-induced influence on the FRD and illustrates how the pattern can be used to determine the locations and sizes of leaks within the system.

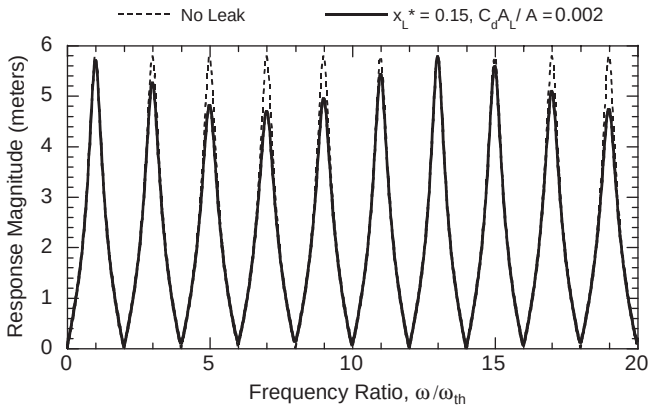

Fig. 2. FRD of the intact and a leaking pipeline shown in Fig. 1.

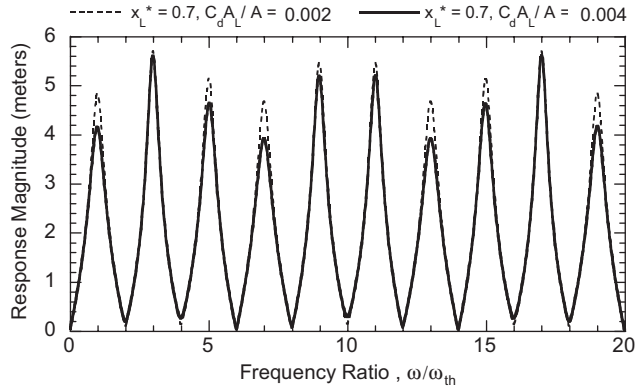

Fig. 3. FRD of the pipeline shown in Fig. 1 with a leak of varying size at $x_L^* = 0.7$.

3. Derivation of the single pipeline frequency response equations

The frequency response of a single pipe can be evaluated numerically using the method of characteristics where a set of hyperbolic partial differential equations are solved in the time domain for the head and discharge at each nodal position in the characteristic grid [20]. The time series data can be translated into the frequency domain through basic signal-processing tools such as the Fourier transform. For an arbitrary signal, the frequency response function of the pipeline is defined as

$$H(\omega) = \frac{R_{xy}}{R_{xx}}, \tag{2}$$

where $H(\omega) =$ frequency response function and $R_{xy}(\omega) =$ Fourier transform of the cross-correlation function between x and y, which stand for input and output, respectively [13].

The method of characteristics is a proven method of transient analysis that can reproduce results that closely replicate experimental data with the use of an appropriate unsteady friction model. The computational time of finely discretized runs, however, can be large for the determination of the FRD. The time–space discretization grid employed in the method of characteristics also limits the number of frequencies that can be represented within the model.

As an alternative to the method of characteristics for frequency response analysis, the unsteady partial differential equations of continuity and momentum are linearized, and variables of head and discharge assumed to oscillate about a mean value [19,20]. Given that the magnitude of the valve perturbation generating the transient is small, close matches can be achieved between the fully nonlinear MOC model and the linearized equations [10]. The solution of the resultant linear equations is arranged in a matrix form to provide the relationship between the upstream and downstream head and discharge responses in the frequency domain. For a pipe element, the transfer matrix solution is

$$\begin{Bmatrix} q \\ h \end{Bmatrix}^{n+1} = \begin{bmatrix} \cosh(\mu l) & -\frac{1}{Z}\sinh(\mu l) \\ -Z\sinh(\mu l) & \cosh(\mu l) \end{bmatrix} \begin{Bmatrix} q \\ h \end{Bmatrix}^{n}, \tag{3}$$

where q, h = discharge and head perturbation and are complex functions of the position with the pipe, x, $Z = (\mu a^2)/(\mathrm{i}\omega g A)$ (the characteristic impedance for the pipe section), superscript n denotes the node number within the system (n and $n+1$ as the upstream and downstream nodes, respectively), $a =$ wave speed, $D =$ diameter, $g =$ gravitational constant, $A =$ area, and $\omega =$ angular frequency of the perturbation. The propagation function is $\mu = (l/a)\sqrt{-\omega^2 + \mathrm{i}gA\omega R}$, where $l =$ length of the uniform pipe section under consideration and $\mathrm{i} = \sqrt{-1}$. $R =$ frictional resistance term, equal to $(fQ_0)/(gDA^2)$ for turbulent flows or $(64\nu)/(gAD^2)$ for laminar flows, where $\nu =$ kinematic viscosity.

Similar matrices may be derived for other pipeline components such as inline and side discharge valves. The transfer matrix for an excitation inline valve in the pipeline is given as [20]

$$\begin{Bmatrix} q \\ h \end{Bmatrix}^{n+1} = \begin{bmatrix} 1 & 0 \\ -\dfrac{2\Delta H_{V0}}{Q_{V0}} & 1 \end{bmatrix} \begin{Bmatrix} q \\ h \end{Bmatrix}^{n} + \begin{Bmatrix} 0 \\ \dfrac{2\Delta H_{V0}\Delta\tau}{\tau_0} \end{Bmatrix}, \tag{4}$$

where ΔH_{V0}, Q_{V0} = the steady-state head loss across and flow through the valve, respectively, τ_0 is the dimensionless valve-opening coefficient at steady state, $\Delta\tau$ = the magnitude of the dimensionless valve-opening perturbation generating the transients. The transfer matrix for a leak [10],

$$\begin{Bmatrix} q \\ h \end{Bmatrix}^{n+1} = \begin{bmatrix} 1 & -\dfrac{Q_{L0}}{2H_{L0}} \\ 0 & 1 \end{bmatrix} \begin{Bmatrix} q \\ h \end{Bmatrix}^{n}, \tag{5}$$

where Q_{L0} and H_{L0} are the steady-state discharge and head at the leak. These matrices, along with the pipe matrices, can be arranged to represent the system under consideration and multiplied together from the downstream to upstream boundary to form an overall transfer matrix between conditions at the boundaries of the system. The total system is solved subject to boundary conditions for each frequency [9,19,20]. An example of such an overall

transfer matrix is

$$\begin{Bmatrix} q \\ h \\ 1 \end{Bmatrix}^b = \begin{bmatrix} U_{11} & U_{12} & U_{13} \\ U_{21} & U_{22} & U_{23} \\ U_{31} & U_{32} & U_{33} \end{bmatrix} \begin{Bmatrix} q \\ h \\ 1 \end{Bmatrix}^a, \tag{6}$$

where $U_{jk} = j$th row and kth column entry for the overall transfer matrix for the pipeline system and a, b are points denoting the upstream and downstream boundaries of the pipe, respectively. The expanded rows in the matrices are used in the cases where inline or side discharge orifices exist within the system. Note that Eq. (3) is displayed with steady-state friction acting on the pipe. To highlight the impact of a leak on the peaks of the FRD, the steady-state friction is removed for the following derivations. The validity of this approximation will be illustrated later in the paper.

For the derivation of the leak-induced impact on the FRD, first consider an arbitrary pipe bounded by a constant head reservoir on the upstream end, with an overall transfer matrix given by Eq. (6). The excitation of the system occurs at the downstream boundary through the use of an inline valve discharging into a downstream constant-head reservoir. Subscripts a and b are positions corresponding to the supply reservoir and the upstream side of the perturbation valve. Expanding the discharge and head equations of Eq. (6) gives

$$q_b = U_{11}q_a + U_{12}h_a + U_{13}, \tag{7}$$

$$h_b = U_{21}q_a + U_{22}h_a + U_{23}. \tag{8}$$

Using the linearized valve orifice equation shown in Eq. (4) to relate the downstream head and discharge and the upstream boundary condition ($h_a = 0$), Eqs. (4), (7) and (8) can be combined to form

$$h_b = \frac{\dfrac{-2\Delta H_{V0}U_{11}U_{23}}{Q_{V0}U_{21}} + \dfrac{2\Delta H_{V0}U_{13}}{Q_{V0}} - \dfrac{2\Delta H_{V0}\Delta\tau}{\tau_0}}{1 - \dfrac{2\Delta H_{V0}U_{11}}{Q_{V0}U_{21}}}. \tag{9}$$

Eq. (9) gives the general head response for an arbitrary pipe bounded upstream by a reservoir and downstream by a valve discharging into a constant head reservoir. The head h_b is measured at a position just upstream of the excitation valve.

For an intact stretch of uniform pipe between the upstream reservoir and the downstream valve, the entries U_{11}, U_{12}, U_{21}, U_{22} of Eq. (6) are given by Eq. (3), where the expanded entries $U_{31} = U_{32} = U_{13} = U_{23} = 0$ and $U_{33} = 1$. For this situation, Eq. (9) becomes

$$h_b = \frac{2\Delta H_{V0}\Delta\tau}{\tau_0\left(1 + \cot\left(\dfrac{L\omega}{a}\right)\dfrac{2gA\Delta H_{V0}}{iaQ_{V0}}\right)}. \tag{10}$$

At the resonance peaks, the angular frequency is defined as

$$\omega_{\text{th}} = \frac{(2m-1)\pi a}{2L}, \tag{11}$$

where m is a positive integer ($m = 1, 2, 3, \ldots$) that corresponds to the peak number. Substitution of Eq. (11) into Eq. (10) produces

$$h_b = \frac{2\Delta H_{V0}\Delta\tau}{t_0\left(1 + \cot\left(\frac{(2m-1)\pi}{2}\right)\frac{2gA\Delta H_{V0}}{iaQ_{V0}}\right)} \tag{12}$$

and simplifies down to

$$|h_b| = \frac{2\Delta H_{V0}\Delta\tau}{\tau_0}. \tag{13}$$

Eq. (13) describes the FRD peaks for an intact stretch of pipeline and is shown to be frequency independent, indicating that at the resonance frequencies an intact pipe will display equal magnitude responses as is illustrated in Fig. 2.

For the case where a single leak exists within the pipe, Eq. (9) becomes

$$h_b = \frac{-\frac{2\Delta H_{V0}\Delta\tau}{\tau_0}}{1 - \frac{2\Delta H_{V0}\left(\cos\left(\frac{(L_1+L_2)\omega}{a}\right) + \frac{iQ_{L0}a}{2gAH_{L0}}\sin\left(\frac{L_1\omega}{a}\right)\cos\left(\frac{L_2\omega}{a}\right)\right)}{Q_{V0}\left(\frac{Q_{L0}a^2}{2H_{L0}g^2A^2}\sin\left(\frac{L_1\omega}{a}\right)\sin\left(\frac{L_2\omega}{a}\right) - \frac{ia}{gA}\sin\left(\frac{(L_1+L_2)\omega}{a}\right)\right)}}, \tag{14}$$

where L_1 and L_2 are the pipe section lengths upstream and downstream of the leak as illustrated in Fig. 1. At the resonance frequencies given by Eq. (11), Eq. (14) becomes

$$h_b = \frac{-\frac{2\Delta H_{V0}\Delta\tau}{\tau_0}}{1 - \frac{\frac{i2\Delta H_{V0}Q_{L0}}{2H_{L0}}\sin\left(x_L^*(2m-1)\frac{\pi}{2}\right)\cos\left((1-x_L^*)(2m-1)\frac{\pi}{2}\right)}{Q_{V0}\left(\frac{Q_{L0}a}{2H_LgA}\sin\left(x_L^*(2m-1)\frac{\pi}{2}\right)\sin\left((1-x_L^*)(2m-1)\frac{\pi}{2}\right) - i\right)}} \tag{15}$$

and $x_L^* = L_1/(L_1 + L_2)$. Using the trigonometric product identities to convert the product of the sine and cosine functions into a summation of the arguments, Eq. (15) becomes

$$h_b = \frac{-\frac{2\Delta H_{V0}\Delta\tau}{\tau_0}}{1 - \frac{2\Delta H_{V0}\left(\frac{iQ_{L0}}{4H_{L0}}\left((-1)^{m+1} + \sin\left(2x_L^*(2m-1)\frac{\pi}{2} - (2m-1)\frac{\pi}{2}\right)\right)\right)}{Q_{V0}\left(\frac{Q_{L0}a}{4H_LgA}\cos\left(2x_L^*(2m-1)\frac{\pi}{2} - (2m-1)\frac{\pi}{2}\right) - i\right)}}. \tag{16}$$

Converting the arguments of the sine and cosine functions into a product of trigonometric functions with the arguments, $x_L^*(2m-1)\pi$ and $(2m-1)\pi/2$, the expression now simplifies

down to

$$h_b = \frac{-\dfrac{2\Delta H_{V0}\Delta\tau}{\tau_0}}{1 - \dfrac{2\Delta H_{V0}\left(\dfrac{iQ_{L0}}{4H_{L0}}\left((-1)^{m+1} + (-1)^m \cos\left(2\pi x_L^* m - \pi x_L^*\right)\right)\right)}{Q_{V0}\left(\dfrac{(-1)^{m+1}Q_{L0}a}{4H_{L0}gA}\sin\left(2\pi x_L^* m - \pi x_L^*\right) - i\right)}}. \tag{17}$$

To further simply the equation, the coefficient of the term Q_{V0} can be shown as approximately constant for reasonable leak sizes. For a wave speed equal to $1200\,\mathrm{m\,s^{-1}}$ and dimensionless leak sizes ($C_d A_L/A$) less than 2×10^{-3} and head at the leak greater than 50 m, the size of $(Q_{L0}a)/(4H_{L0}gA)$ is smaller than 0.05. Therefore, under realistic combinations of leak size and head at the leak the coefficient of Q_{V0} (in brackets) in Eq. (17) can be approximated by the constant "$-i$". Note that this combination of leak size and head at the leak results in a discharge out of the leak that is equivalent to 28.5% of the base flow and forms the upper limit of plausible leak sizes and driving head conditions. The head response magnitude becomes

$$|h_b| = \frac{1}{\dfrac{\tau_0}{2\Delta H_{V0}\Delta\tau}\left(1 + \dfrac{2\Delta H_{V0}}{Q_{V0}}\left(\dfrac{Q_{L0}}{4H_{L0}}\left(1 + \cos\left(2\pi x_L^* m - \pi(1 + x_L^*)\right)\right)\right)\right)}. \tag{18}$$

The physical interpretation of the approximation is akin to neglecting all higher order reflections from the leak (e.g. those generated by multiple reflections off the leak). The form of Eq. (18) indicates that the magnitude of the FRD at resonance frequencies for a leaking pipe is no longer given by the constant in Eq. (13) but varies in an inverted sinusoidal form. This sinusoidal pattern is the imposed leak pattern illustrated in Refs. [11,12,18]. The major component of the pattern in Eq. (18) has a frequency in terms of the resonance peak number, m, of x_L^*, a phase of $\pi(1 + x_L^*)$ and a magnitude of $(Q_{L0}\tau_0)/(4\Delta\tau Q_{V0}H_{L0})$. The analysis of the pattern can, therefore, yield information concerning the location and the size of the leak. Care is needed, however, before the results of Eq. (18) can be directly applied, as Eq. (18) is valid only at each resonance frequency and occurs in the denominator of Eq. (18). The theoretical sinusoidal pattern imposed by the leak is therefore acting on the inverted peak magnitudes and sampled with a frequency $1/m = 1$, giving a Nyquist threshold of $1/m = 0.5$. As the value of x_L^* will range between 0 and 1, this implies that for $x_L^* > 0.5$, the imposed pattern will suffer distortions and the original pattern frequency will manifest itself as a new frequency that is observable within the allowable range $x_L^* = [0, 0.5]$. This process is commonly known as aliasing and the distorted new frequency will be given by

$$\omega'_{\mathrm{signal}} = 2\omega_{\mathrm{nq}} - \omega_{\mathrm{signal}}, \tag{19}$$

where $\omega'_{\mathrm{signal}}$ and ω_{signal} signal are the distorted and the original signal frequencies, respectively, and ω_{nq} is the Nyquist frequency, equal to half the sampling frequency. For down-aliased signals, where $\omega_{\mathrm{signal}} < 2\omega_{\mathrm{nq}}$, the phase of the original signal undergoes a reversal [21]:

$$\phi'_{\mathrm{signal}} = -\phi_{\mathrm{signal}}, \tag{20}$$

where ϕ'_{signal} and ϕ_{signal} are the distorted and original phases of the signal, respectively. From Eq. (18), the observed frequency in the leak-damping pattern is the dimensionless leak position. As the leak-induced pattern is sampled at every resonance peak, the sampling frequency is given by $1/m = 1$ and the Nyquist frequency is $1/m = 0.5$. For leak positions beyond the midpoint of the pipe, the leak-induced pattern is always aliased. The influence of aliasing on the leak-induced pattern on the FRD is that for each observed leak-induced pattern there are two possible frequencies—and hence two leak positions—located at symmetric positions within the pipe, as given by Eq. (19). One leak position is associated with a frequency below the Nyquist frequency of $1/m = 0.5$, and is located in the upstream half of the pipe, and the other above the Nyquist frequency, corresponding to the downstream half of the pipe. The phase of the observed signal can be used to determine whether the original leak imposed signal has been aliased. From Eq. (18) the phase of a signal with $\omega_{\text{signal}} < \omega_{\text{nq}}$ is $\pi(1 + x_L^*)$ and is located between $-\pi < \phi < -\pi/2$. For an aliased signal, the phase becomes $-\pi(1 + x_L^*)$ and is in the range of $0 < \phi < \pi$. The properties of the leak-induced pattern are as follows:

- The frequency of the leak-induced damping pattern is x_L^* or $(1 - x_L^*)$.
- The phase of the leak-induced damping pattern is $\pm\pi(1 + x_L^*)$ and is located in the third quadrant of the unit circle when the leak is in the upstream half of the pipe and in the first quadrant when the leak is located in the downstream half.
- The magnitude of the leak-induced pattern is $(Q_{L0}\tau_0)/(4\Delta\tau\, Q_{V0}H_{L0})$, given in Eq. (18) as the coefficient to the leak-generated cosine function.

The extraction of the observed leak-induced pattern properties can be performed by applying a Fourier transform to a set of data containing the magnitude of the resonance peaks in the FRD. The magnitudes should be inverted to allow an accurate extraction of sinusoidal function in the denominator of Eq. (18).

4. Procedure for leak location and sizing

The results from the above derivations can be used in two different ways to detect leaks in a pipe: the peak-coding method [12], or by direct Fourier analysis. The peak-coding method involves the prior generation of the coding table, which contains the peaks sequence ranked in order of magnitude for each leak position. Coding tables can be generated using Eq. (18) by varying the location of a leak in a single pipeline and for each leak location determining the value of the cosine function within Eq. (18) for a required number of harmonic frequencies. The inverted values of the cosine function are representative of the relative sizes between resonance peaks of different harmonics and can then be ranked and combined to form a numerical coding and tabulated with the leak location. Each coding provides a sequence of numbers that describes the leak-induced pattern in the FRD. The sequence observed in the real pipeline can be matched to sequences presented in the table to find the location of the leak without complicated analysis. The purpose of the coding is to provide a numerical summary of the shape of the FRD. The exact way in which this coding is performed is arbitrary as long as the shape of the FRD is fully summarized within the coding system [10]. The number of resonance peaks used in the coding, however, determines the resolution of the leak detection process. For a coding sequence involving

three resonance peaks, a leak can be located in a region that is approximately 16% of the total pipe length. Increasing the numbers of resonance peaks further to 6 and 25 increases the resolution to 3.6% and 0.2%, respectively. The advantage of using the coding technique is that once the table has been generated for a particular pipe, no further calculation is needed to locate the leak from the FRD. The disadvantage is that while it provides a good indication of the location of the leak, such tables cannot be used to determine the magnitude of the leak. Further information concerning the use of the coding tables can be found in Ref. [12].

Alternatively, the frequency of the leak-induced pattern on the peaks can be extracted directly through Fourier decomposition. The procedure is as follows:

1. Perform a Fourier transform on the data containing only the inverted response at each resonant frequency (the peaks) in the FRD and identify the major frequency, f, within the damping pattern of the response. The dimensionless leak location, x_L^*, is either f or $1-f$.
2. Determine the phase of the major frequency to find which side of the pipe the leak resides. For phase located in between $-\pi<\phi<-\pi/2$, the corresponding peak is located at $x_L^*<0.5$. For phase located in $0<\phi<\pi$, the corresponding peak is located at $x_L^*>0.5$.
3. In conjunction with the location of the leak, the discharge and steady-state head at the leak can be calculated from the magnitude of the oscillation and is equal to $(Q_{L0}\tau_0)/(4\Delta\tau Q_{V0}H_{L0})$, given in Eq. (18). The lumped leak parameter is determined using the known steady flow through the valve, the magnitude of the valve perturbation, and the orifice equation,

$$Q_{L0} = C_d A_L \sqrt{2gH_{L0}}. \tag{21}$$

The validity of this leak detection procedure is illustrated in the following example. Although the leak-induced pattern from the peak magnitudes of the FRD can be performed in a straightforward fashion using the Fourier transform (FT), the FT requires a significant number of data points to produce a high-resolution frequency spectrum. The bandwidth of the input signal often limits the number of resonance peaks that can be observed in the FRD. Alternatively, the extraction process can be taken in two discrete steps, where the first step uses the FT to determine a rough estimate of the frequency and phase of the leak-induced pattern and the second step uses the results from the first step as an initial guess to a least-squares regression between the observed peak magnitudes and a sinusoidal function. For illustrative purposes, however, the following numerical examples use the Fourier transform of a large number of peak responses (4096) to give a clear illustration of the spectrum of the leak-induced pattern. Fig. 4 contains the Fourier decomposition of the inverted peak magnitudes in the FRD of the pipe in Fig. 1 for four situations where the same-sized leak ($C_dA_L/A = 2\times10^{-3}$ or 15 mm diameter leak with $C_d = 0.8$) is located at different positions along the pipe. The size of the valve perturbation is kept small (10% of the original valve-opening size) to ensure linear system behaviour [10].

The relative phases and magnitudes of the lumped leak parameter for each situation are displayed in Table 2. For all cases where $x_L^*<0.5$, the Fourier transform results indicate that the leak-induced frequency is equal to x_L^*. For the situation where $x_L^* = 0.862$, the pattern has a frequency of $(1-x_L^*)$, as predicted by Eq. (19). The pattern frequency is the same between the two mirrored positions, $x_L^* = 0.138$ and 0.862. To determine in which half of the pipe the leak resides, the phase of the patterns needs to be taken into account. From Table 2, the phases of all leak cases where $x_L^*<0.5$ are within $-\pi<\phi<-\pi/2$, and it is only for the situation where $x_L^* = 0.862$ that

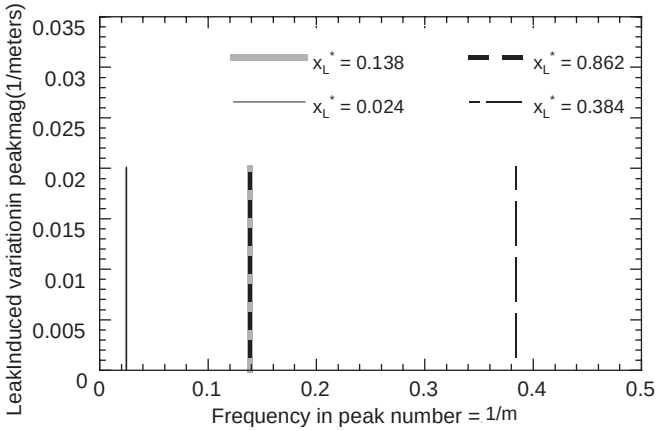

Fig. 4. Fourier decomposition of inverted peak magnitudes in the FRD of the same leak in four different locations.

Table 2
Predicted leak location, phase of leak-induced patterns and predicted leak magnitude

Actual leak location x_L^*	Predicted leak location x_L^*	Phase (rad)	$C_d A_L/A$
0.138	0.138	−2.707	0.002
0.024	0.024	−3.065	0.002
0.862	0.862	0.438	0.002
0.384	0.384	−1.934	0.002

the phase of the pattern lies within $0<\phi<\pi$, indicating that the leak is located at the downstream half of the pipe. The magnitude of the frequency spike for all four leak positions is equal to $0.02\,\mathrm{m}^{-1}$. To determine the steady-state impedance of the leak, the steady-state discharge through the valve needs to be known and for the flow parameters displayed in Table 1, this flow, Q_{V0}, is $0.011\,\mathrm{m}^3\,\mathrm{s}^{-1}$. Following the procedure set out in step 3 above, the steady-state driving head at the leak and the steady-state discharge through the leak can be determined from the HGL and the magnitude of the frequency spikes in Fig. 4, respectively. As the leak is assumed to be small, the value of the HGL at the leak position can be approximated by a linear interpolation between the reservoir head and the head upstream of the valve. The substitution of these values into Eq. (21) gives the dimensionless lumped leak parameter that corresponds to the true value set out in Table 1 for all four situations.

The leak detection procedure set out above can be used to accurately locate and size leaks within a pipe. Note that the FRD of the four case studies were produced numerically from a friction-affected system. The correspondence between true and predicted leak size and position values highlights the validity of Eq. (18) even though it was derived based on a frictionless assumption. The detailed discussion on the impact of steady and unsteady friction on the results will be presented later in the paper. In the following section, the above procedure is further expanded to multiple leak situations.

5. Derivation of multiple leak damping pattern on FRD

Following the procedure for a single leak, an equivalent expression for Eq. (17) for multiple leaks in the pipe is

$$h_b = \frac{-\dfrac{2\Delta H_{V0}\,\Delta\tau}{\tau_0}}{1-\dfrac{2\Delta H_{V0}\left(\sum_{k=1}^{n_{\text{Leak}}}\left[\dfrac{iQ_{L0}^{k}}{4H_{L0}^{k}}\left((-1)^{m+1}+(-1)^{m}\cos(2\pi x_L^{k^*}m-\pi x_L^{k^*})\right)\right]\right)}{Q_{V0}\left(\sum_{k=1}^{n_{\text{Leak}}}\left[\dfrac{(-1)^{m+1}Q_{L0}^{k}a}{4H_{L0}^{k}gA}\sin(2\pi x_L^{k^*}m-\pi x_L^{k^*})\right]-i\right)}}, \tag{22}$$

where n_{Leak} is the number of leaks in the system, $x_L^{k^*}$ the distance of the kth leak from the upstream boundary divided by the total length of the pipe, and the superscript k denotes the parameter for the kth leak.

For the multiple leak situation the coefficient of Q_{V0} can only be assumed as the constant $-i$ when

$$\sum_{k=1}^{n_{\text{Leak}}}\left[\frac{Q_{L0}^{k}a}{4H_{L0}^{k}gA}\right]\ll 1. \tag{23}$$

Under this assumption, Eq. (22) becomes

$$|h_b| = \frac{1}{\dfrac{\tau_0}{2\Delta H_{V0}\Delta\tau}\left(1+\dfrac{2\Delta H_{V0}}{Q_{V0}}\sum_{k=1}^{n_{\text{Leak}}}\left[\dfrac{Q_{L0}^{k}}{4H_{L0}^{k}}\left(1+\cos\left(2\pi x_L^{k^*}m-\pi(1+x_L^{k^*})\right)\right)\right]\right)}. \tag{24}$$

Eq. (24) now shows that the leak-induced pattern now consists of n_{Leak} different sinusoidal functions. Fig. 5 shows the Fourier decomposition of the inverted response upstream of the valve

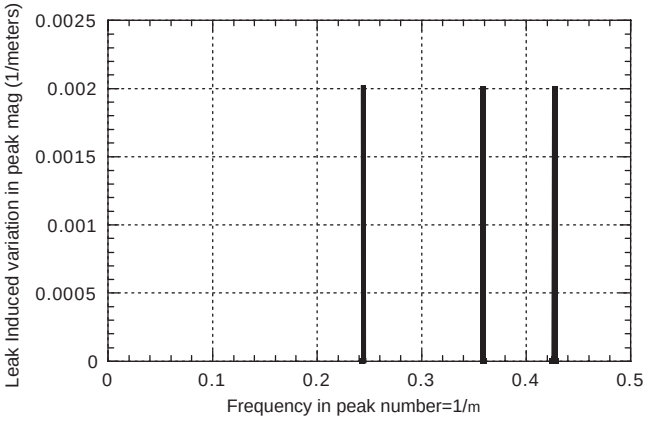

Fig. 5. Fourier decomposition of leak-imposed damping pattern on the FRD of a single pipe containing three leaks simultaneously.

Table 3
Predicted leak locations, phases of leak-induced patterns and predicted leak magnitudes

Actual leak location x_L^*	Predicted leak location x_L^*	C_dA_L/A	Phase (rad)
0.244	0.244	0.0002	−2.375
0.427	0.427	0.0002	−1.799
0.641	0.641	0.0002	1.129

when three leaks ($x_L^* = 0.244,\ 0.427,\ 0.641$) of the same size ($C_dA_L/A = 2 \times 10^{-4}$, or 1.5 mm diameter leak for $C_d = 0.8$) are located simultaneously in the pipe. The sizes of the leaks have been reduced from the previous example to satisfy the conditions of Eq. (23), and from previous discussion the combined discharges out of the leaks can be as large as 30% of the base flow before Eq. (23) is violated. The Fourier decomposition of Fig. 5 shows spikes at all the correct frequencies with correct phase and magnitude, thus identifying all three leaks simultaneously. The summary of the multi-leak results is shown in Table 3 and illustrates how the technique may also be applied to locate and size accurately multiple leaks within a single pipeline. The following sections discuss issues concerning the physical application of this technique and limitations of the method.

6. Impact of friction

In the derivation of the expression for the leak-induced pattern, both steady and unsteady friction effects are ignored to highlight the impact of the leak on the peaks of the FRD. The following section discusses the impact of both steady and unsteady frictions on the FRD.

6.1. Impact of steady friction

An impact of steady-state friction on the FRD is twofold:

1. It reduces the overall magnitude of the frequency response (frequency-independent damping).
2. It induces a difference in impedance between pipe sections of different steady frictional resistance, R, from the different flows in pipe sections either side of the leak.

The investigation of the first impact was conducted by generating the FRD for the intact pipeline of Fig. 1 under increasing pipe roughness with the relative roughness, ε/D, ranging from a value of 0 to 0.017. A comparison of the FRD between different values of ε/D is shown in Fig. 6. For each value of relative roughness, the standard deviation of the first 20 resonance peaks in the FRD was used as a measure of any frictionally induced pattern on the FRD. The standard deviation was found to be less than 10^{-10} and is likely caused by small rounding-off error, and is confirmation that steady friction is not a frequency-dependent phenomenon and will not distort the leak-induced pattern. This can also be seen in Fig. 6 where the magnitudes of the peaks in the FRD are reduced uniformly as a result of increasing steady friction.

The second impact of steady-state friction on the FRD is that the characteristic impedance between sections of adjacent pipes with different flows (e.g. separated by a leak) is not equal due

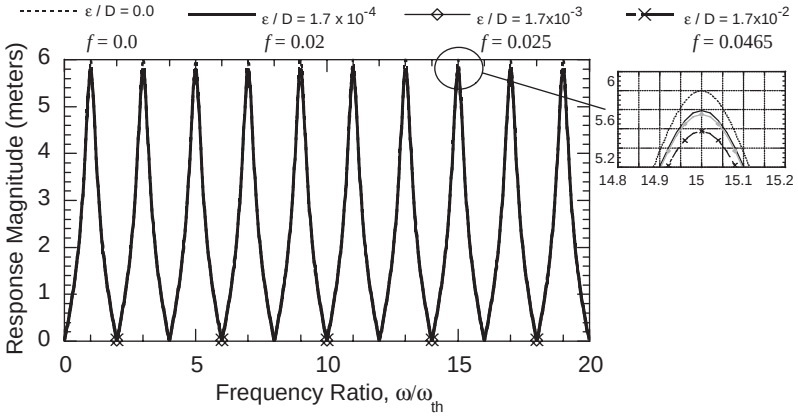

Fig. 6. Impact of steady-state friction on the FRD.

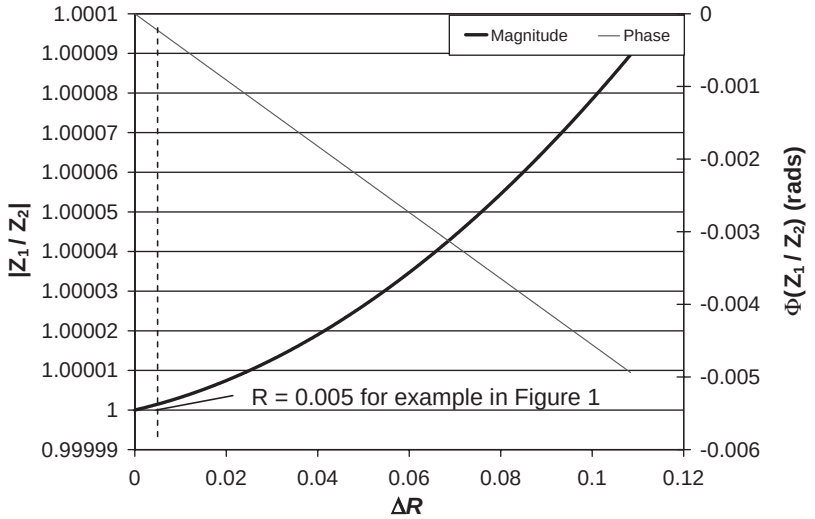

Fig. 7. Values of $|\mu_1/\mu_2|$, $\phi(\mu_1/\mu_2)$ with ΔR in the pipes upstream and downstream of a leak for system in Fig. 1.

to the difference in discharges between each section. Such a difference in impedance is reflected in the FRD as a shift in the frequency of the resonance peaks and has been used to determine the location and sizes of extended blockages and leaks in air pipes [22–26]. Fig. 3 shows, however, that any such leak-induced changes in impedance for $C_d A_L/A < 4 \times 10^{-3}$ are negligible in liquid pipelines. This was also illustrated in publication [18].

Fig. 7 shows the impact of steady friction on the magnitude and phase (ϕ) ratios of the characteristic impedance function, Z, for pipe sections located upstream and downstream of a midpoint leak in the system of Fig. 1. The figures are generated by gradually increasing the flow difference between the two pipe sections and the corresponding mean characteristic impedance function ratio (Z_1/Z_2) for the first 20 resonance peaks in the FRD is calculated. The ratio of the characteristic impedance function is plotted against the difference in frictional pipe resistance

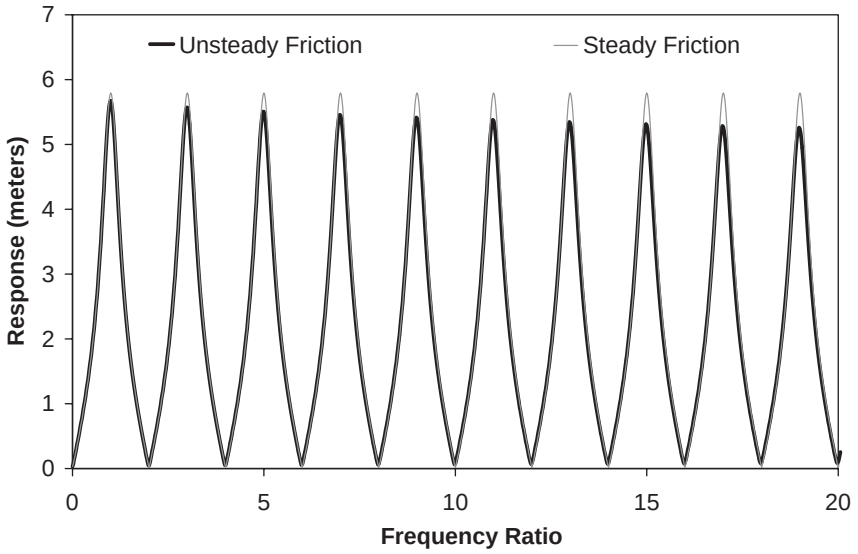

Fig. 8. Comparison between results with and without unsteady friction for the intact pipeline of Fig. 1.

factor, ΔR, between the two pipe sections. This resistance factor difference provides an indication of the leak flow rate, and larger values of ΔR indicate a larger leak. For all values of ΔR considered, the change in characteristic impedance between pipe sections is negligible. For the flow conditions and leak size shown in Table 1, the value of ΔR is 5.03×10^{-3}, corresponding to a difference of characteristic impedance less than 10^{-3}%. The figure therefore indicates that the characteristic impedance upstream and downstream of the leak is nearly identical for all reasonable leak sizes.

From the above analysis, it may be concluded that steady-state friction has a minimal impact on the shape of the FRD for the range of leak sizes and pipe roughness heights considered and can be safely removed from the future derivations.

6.2. *Impact of unsteady friction*

Unsteady friction is a phenomenon that occurs in pipes as a result of abrupt changes in the velocity profile during unsteady flow. The impact of unsteady friction is frequency dependent. Publication [27] shows expressions for the existing unsteady friction models [28,29] in the frequency domain. Unlike steady-state friction, unsteady friction induces non-uniform changes in the magnitude of the resonant peaks in the FRD, thus requiring a modification in the proposed leak location method to operate successfully. Fig. 8 shows the comparison between steady and combined steady and unsteady friction FRD results for the leak-free system of Fig. 1 using the unsteady friction model from Ref. [29]. A negative trend in the FRD peak magnitudes is observed in the case with unsteady friction. To deal with unsteady frictional effects in real pipes, an array of scaling factors can be derived numerically for a leak-free case between pure steady friction and unsteady friction results such that the unsteady friction effects can be eliminated from the

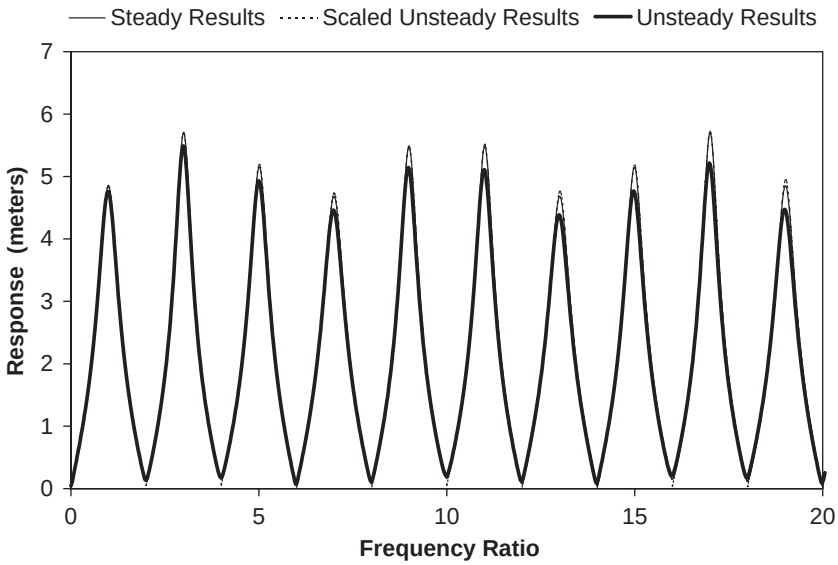

Fig. 9. Results of corrected unsteady friction FRD with steady friction FRD with the scaled unsteady are identical to the steady friction result.

experimentally derived FRD prior to the application of the leak detection method. The scaling factors are ratios between the steady and unsteady friction FRD results at the frequencies of interest,

$$\mathrm{SF}(\omega) = \frac{h_S(\omega)}{h_{U+S}(\omega)}, \tag{25}$$

where SF = scaling factor, h_S = response under steady friction and h_{U+S} = response under combined steady and unsteady friction. Fig. 9 shows the steady and unsteady FRD results from the leaking pipe of Fig. 1, with $x_L^* = 0.7$. The scaled FRD, using scaling factors derived from Eq. (25), is also shown on the figure and effectively matches the results under steady friction alone. The use of scaling factors derived numerically from a leak-free pipeline to correct results from a real pipeline that potentially contains leaks assumes that the effect of steady and unsteady friction is the same for both cases. Such an assumption is only valid for a range of leak sizes where the impedances of the sections of pipe upstream and downstream of the leak are similar. The magnitude and phase ratios of the impedance between the upstream and downstream pipe sections from a leak located at the midpoint of the pipe in Fig. 1 for varying flow difference and combined steady and unsteady friction is shown in Fig. 10. These results are averaged between the first 20 resonance peaks in the FRD. The results closely resemble those of Fig. 7, indicating that for a difference in flow conditions generated by small leaks, the unsteady friction induced difference in impedance is negligible. The scaling technique is, therefore, a valid method of compensating for unsteady friction in a real pipeline situation.

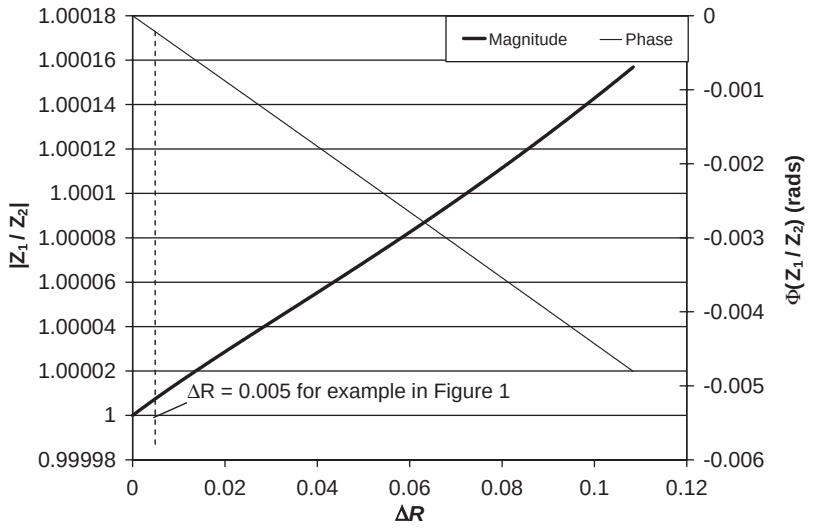

Fig. 10. Values of $|\mu_1/\mu_2|$, $\phi(\mu_1/\mu_2)$ with ΔR for combined unsteady and steady frictions for the system in Fig. 1, phase values in radians.

7. Implementation of the technique

The proposed method of leak detection hinges on the accurate extraction of the FRD from the pipe, possible issues that can arise during practical implementation need to be addressed before use can be made of the results presented in the previous section.

7.1. Methods of FRD extraction

The methodology of frequency response extraction has been covered extensively by publications in the past. Two techniques are commonly used for this purpose: the frequency sweep [20] and the use of linear systems theory [9–13]. The frequency sweep involves the sequential injection of monotone sinusoidal signals in the pipeline through oscillating hydraulic elements such as oscillating valves [20]. The magnitude of the resultant pressure oscillations is measured and plotted against the input signal frequency to obtain the full FRD. The main problem with the frequency sweep technique is that the time required to generate FRDs of good resolution may take many hours, depending on the length of the pipe in question.

Alternatively, techniques that take advantage of linear systems behaviour are more time efficient. Pipes under the influence of small-amplitude pressure transients can be approximated as linear systems where all frequencies in the input signal (e.g., the perturbation of the valve opening) behave independently of each other. Each injection of a complex waveform into the pipe may be considered as a simultaneous injection of a multitude of sinusoidal signals into the pipe. The amplitude of each sinusoidal signal is affected according to the frequency response of the pipe. The pressure trace measured from the injection of a wide-band signal, for example, a sharp impulse, is equivalent to the summation of the responses from hundreds of monotone sinusoidal

injections. Thus, the method is a much faster way of determining the response from the pipe for a large number of frequencies. The FRD from such an operation is determined by measuring both the input and output signals and applying Eq. (2). For example, the FRD upstream of the valve in Fig. 1 can be determined by a controlled perturbation of the downstream valve and measuring the subsequent head response at that point. While the shape of the input signal used for this application is arbitrary, care must be taken such that the magnitude of the signal does not violate linearity assumptions, the distortional impact of which is shown in Ref. [9]. Another significant advantage of using Eq. (2) for FRD extraction is that the correlation process actively reduces the effect of random background noise from the data, further increasing the practicality of the technique.

Ref. [12] has shown time series results produced using the method of characteristics where a pseudo-random binary perturbation of an inline downstream valve and Eq. (2) were used to generate the FRD for the single pipe in Fig. 1. The resultant FRD was shown to correspond with both results generated from a typical frequency sweep and the results from the transfer matrix equation.

7.2. *Influence of system configuration*

The equations describing the leak-induced damping pattern on the FRD are derived for a typical reservoir–pipe–valve–reservoir system. The excitation is assumed to be a result of an inline valve perturbation and the pressure measured at a point located just upstream of the valve, which is the optimum measurement position as described Lee et al. [12]. A deviation from this configuration results in the distortion of the FRD, and while inline valves are typically located at the downstream boundary for flow control and can be adapted for transient generation, the existence of a tapping point just upstream of this valve for the insertion of a pressure transducer may not be possible in some cases. Strategies for dealing with the output measurement located away from the optimum point are needed in these situations. Two different schemes are developed to transfer the measured head response at a point within the pipe to the point just upstream of the valve. Both schemes require that the stretch of pipeline between the measurement point and the valve is intact or that the transfer matrix between the two is exactly known.

- Scheme 1—By taking advantage of the known valve boundary conditions, direct transfer using the valve orifice equation can be carried out. Eqs. (3) and (4) are combined to form a set of equations where h_n, q_n are the complex head and discharge perturbation at the measurement point and h_{n+1}, q_{n+1} are the complex head and discharge perturbation upstream of the valve, respectively. Note that h_n is the only known parameter and is measured from the pipe. Rearranging the equations gives

$$h_{n+1} = \frac{-\dfrac{T_{11}T_{22}}{T_{21}}h_n + T_{12}h_n - \dfrac{Q_{V0}\Delta\tau}{\tau_0}}{\dfrac{Q_{V0}}{2\Delta H_{V0}} - \dfrac{T_{11}}{T_{21}}}, \tag{26}$$

  where T is the transfer matrix for the stretch of intact pipe joining the measurement position and the perturbation valve, the entries of which are given by Eq. (3).

- Scheme 2—Transfer between two measurement points. For this scheme, two measurement points are needed, preferably close together, such that the section of pipe between the points can be verified as leak-free. Eq. (3) can be used to determine the discharge response at one of the measurement points and then reapplied to determine the head response upstream of the inline valve. The advantage of this scheme over scheme 1 is that the steady-state discharge at the valve, Q_{V0}, does not need to be known. The overall transfer equation for scheme 2 is

$$h_{n+2} = T_{21}^{b}\left[T_{11}^{a}\left(\frac{h_{n+1} - T_{22}^{a}h_n}{T_{21}^{a}}\right) + T_{12}^{a}h_n\right] + T_{22}^{b}h_{n+1}, \tag{27}$$

  where T^a, T^b are transfer matrices for the intact pipes between the first and second measurement points and the second measurement point to the perturbation valve. The entries of both T^a, T^b can be determined from Eq. (3). Note that the "first" measurement point is the more upstream of the two measurement points. h_n, h_{n+1} are the measured complex head responses at the first and second measurement points, and h_{n+2} is the transferred head response upstream of the valve.

The validity of both schemes is illustrated in the following example. The FRD of the pipe in Fig. 1 is measured using two different pressure transducers located at 60 and 50 m upstream of the valve. The original pressure responses are measured at both transducers with the target being to calculate the response at the valve. Fig. 11 shows the Scheme 1 transferred response using the 50 m transducer and Eq. (26), also the scheme 2 transferred response using both transducers and Eq. (27) and the true response at the valve. Both schemes were found to transfer accurately the original response to the new position at the valve.

7.3. Application to more complex networks

The technique presented in this paper has been derived for a single pipeline system bounded by a reservoir and an inline excitation valve. The extension of this technique into more complex piping systems consisting of multiple series pipes or pipe networks is important. A technique of

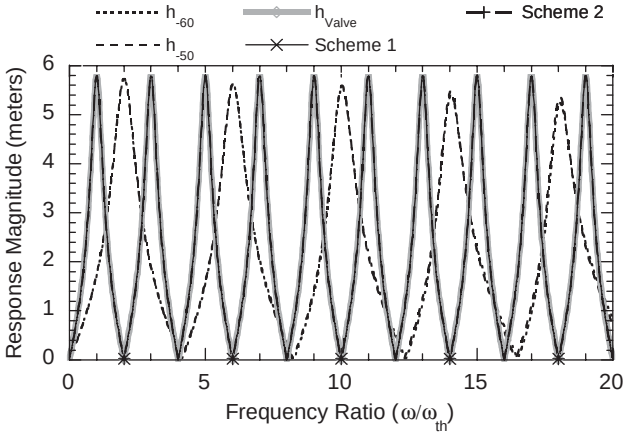

Fig. 11. Results of the measurement transfer schemes in Eqs. (26) and (27).

subdividing complex systems into individual single pipes is presented in Ref. [12], where the FRD of each individual pipe segment can be extracted and the technique presented above be used to determine pipe integrity.

8. Limitations of the method

The proposed method for leak detection in the frequency domain has a number of minor limitations. For example, the fact that leak-induced patterns are aliased and phase reversed means that two leaks located at perfect symmetric positions of the pipeline will manifest themselves as a single leak, and leaks located exactly at the mid-point of the pipe will be undetected. In addition, the estimation of leak size is dependent upon the accuracy of the steady-state discharge measurement out of the downstream valve. While in most cases rudimentary flow measurement devices exist within the systems, the accuracy of these devices varies and can result in poor estimation of the true leak magnitude. The generation of the transient using an inline valve also imposes a limitation on the head difference at the system boundaries. In cases where the heads at both boundaries are equal (static system), the perturbation of the inline valve will not induce a change in flow within the system and a transient cannot be produced. Finally, as linearized equations are used in these derivations, care must be taken so the perturbation transients are not of a magnitude that violates the linear assumption.

9. Conclusions

The frequency response diagram of an intact (leak free) pipe consists of a series of equally spaced peaks that are of either equal magnitudes for steady friction-dominated systems or smoothly decreasing peaks for unsteady friction-dominated systems. The magnitudes and locations of these peaks are determined by the pipe parameters such as length, roughness, wave speed and boundary conditions. The presence of leaks results in a change in the behaviour of the system, which manifests itself as an oscillatory pattern on the frequency response diagram of the system. As a result, leaks can be identified using this pattern, and without the need for a prior "leak-free" response for comparison.

An analytical expression for the leak-induced pattern has been derived from the linearized unsteady equations of continuity and motion, along with the orifice equations associated with leaks and valves. The frequency and phase of the leak-induced pattern at the resonant peaks of the FRD are used to determine the exact location and size of the leak within the pipeline. The leak detection technique is shown to be valid for cases where multiple leaks exist simultaneously within the system, such that the size and location of each individual leak can be determined accurately using the derived expressions. The leak detection technique is well suited for real-time pipeline monitoring using small-amplitude transients that do not impose significant changes to the original flow conditions and for leaks that lose less than 30% of the total flow through the system. A similar set of expressions can be derived for the detection, location and sizing of discrete blockages.

The use of linear system theory and the simultaneous measurement of the input signal (valve opening) and the output signal (head response at the valve) is suggested for the fast and accurate extraction of the FRD without potential harm to the system. Two schemes were derived for dealing with the problem of measurement positions that are located away from the optimum measurement point (at the valve). Both showed the ability to transfer the response from any position within the pipe to a position just upstream of the valve, provided that the section of pipe between the original measurement points and the valve is known to be leak free. The impact of unsteady friction, using the Vardy and Brown [29] model, was investigated and found to induce an additional trend to the peaks of the FRD. This trend can be removed using numerically determined scaling factors.

The proposed technique is the first comprehensive technique of leak detection using the FRD, which is able to detect both single and multiple leaks. Given that the technique depends on the nature of the leak-induced pattern of the FRD, the baseline about which this pattern occurs is irrelevant. This clear impact of a leak on the FRD has removed the problem of having to compare results to a known "leak-free" response to determine changes in the system behaviour, and also knowledge of the extent of system friction is no longer required.

References

[1] J.A. Liggett, L.C. Chen, Inverse transient analysis in pipe network, *Journal of Hydraulic Engineering* 120 (8) (1994) 934–955.

[2] J.P. Vítkovský, A.R. Simpson, Calibration and leak detection in pipe networks using inverse transient analysis and genetic algorithms, Research Report No. R157, August, 1997, Department of Civil and Environmental Engineering, University of Adelaide, Australia.

[3] G. Nash, B. Karney, Efficient inverse transient analysis in series pipe systems, *Journal of Hydraulic Engineering* 125 (7) (1999) 761–764.

[4] J.P. Vítkovský, A.R. Simpson, M.F. Lambert, Transients for calibration of pipe roughnesses using genetic algorithms, *Journal of Water Resources Planning and Management* 126 (4) (2000) 262–265.

[5] X.J. Wang, M.F. Lambert, A.R. Simpson, J.A. Liggett, J.P. Vítkovský, Leak detection in pipeline systems using the damping of fluid transients, *Journal of Hydraulic Engineering* 128 (7) (2002) 697–711.

[6] L. Jönsson, M. Larson, Leak detection through hydraulic transient analysis, in: B. Coulbeck, E. Evans (Eds.), *Pipeline Systems*, Kluwer Academic Publishers, Dordrecht, 1992, pp. 273–286.

[7] B. Brunone, Transient test-based technique for leak detection in outfall pipes, *Journal of Water Resources Planning and Management* 125 (5) (1999) 302–306.

[8] D. Covas, H. Ramos, Leakage detection in single pipelines using pressure wave behaviour, *Water Industry System: Modelling and Optimisation Application* 1 (1999) 287–299.

[9] P.J. Lee, J.P. Vítkovský, M.F. Lambert, A.R. Simpson, J.A. Liggett, Leak detection in pipelines using an inverse resonance method, *2002 Conference on Water Resources Planning & Management*, Virginia, USA, 19–22 May 2002.

[10] Lee, Vítkovský, Lambert, Simpson, Liggett, Discussion of "Leak detection in pipes by frequency response method using a step excitation" by W. Mpesha, M. H. Chaudhry, and S.L. Gassman, *Journal of Hydraulic Research* 40(1) (2002) 55–62, in: *Journal of Hydraulic Research* 41(2) (2003) 221–223.

[11] P.J. Lee, J.P. Vítkovský, M.F. Lambert, A.R. Simpson, J.A. Liggett, Frequency response coding for the location of leaks in single pipeline systems, in: *International Conference on Pumps, Electromechanical Devices and Systems Applied to Urban Water Management*, IAHR and IHR, Valencia, Spain, 22–25 April 2003, pp. 371–378.

[12] P.J. Lee, J.P. Vítkovský, M.F. Lambert, A.R. Simpson, J.A. Liggett, Detection of leaks in a fluid pipelines using a linear system transfer function, *Journal of Hydraulic Engineering*, in press.

[13] C.P. Liou, Pipeline leak detection by impulse response extraction, *Journal of Fluids Engineering* 120 (1998) 833–838.
[14] D. Poussart, U.S. Ganguly, Rapid measurement of system kinetics—an instrument for real-time transfer function analysis, *Proceedings of the IEEE* 65 (5) (1977) 741–747.
[15] T. Akiyama, Pressure estimation from oscillatory signals obtained through BWR's instrument lines, *Journal of Dynamic Systems, Measurement and Control* 108 (3) (1986) 80–85.
[16] T. Niederdränk, Maximum length sequences in non-destructive material testing: application of piezoelectric transducers and effects of time variances, *Ultrasonics* 35 (1997) 195–203.
[17] K. Heutschi, A. Rosenheck, Outdoor sound propagation measurements using an MLS technique, *Applied Acoustics* 51 (1) (1997) 13–32.
[18] M. Ferrante, B. Brunone, A.G. Rossetti, Harmonic analysis of pressure signal during transients for leak detection in pressurized pipes, BHR Group, *Fourth International Conference on Water pipeline system—Managing Pipeline Assets in an Evolving Market*, York, UK, 28–30 March 2001.
[19] M.H. Chaudhry, Resonance in pressurized piping systems, *Journal of the Hydraulics Division* 96 (HY9) (1970) 1819–1839.
[20] M.H. Chaudhry, *Applied Hydraulic Transients*, Van Nostrand Reinhold, New York, 1987.
[21] A. Ambardar, *Analog and Digital Signal Processing*, second ed., Brooks/Cole, USA, 1999.
[22] P. Mermelstein, Determination of the vocal-tract shape from measured format frequencies, *The Journal of the Acoustical Society of America* 41 (5) (1967) 1283–1294.
[23] W. Qunli, F. Fricke, Estimation of blockage dimensions in a duct using measured eigenfrequency shifts, *Journal of Sound and Vibration* 133 (2) (1989) 289–301.
[24] W. Qunli, F. Fricke, Determination of blockage locations and cross-sectional area in a duct by eigenfrequency shifts, *Journal of the Acoustical Society of America* 87 (1) (1991) 67–75.
[25] M. De Salis, N. Movchan, D. Oldham, Characterizing holes in duct walls using resonance frequencies, *Journal of the Acoustical Society of America* 111 (6) (2002) 2583–2593.
[26] M.H.F. De Salis, D.J. Oldham, The development of a rapid single spectrum method for determining the blockage characteristics of a finite length duct, *Journal of Sound and Vibration* 243 (4) (2001) 625–640.
[27] J.P. Vítkovský, A. Bergant, A.R. Simpson, M.F. Lambert, Steady oscillatory flow solution including unsteady friction, in: *International Conference on Pumps, Electromechanical Devices and Systems Applied to Urban Water Management*, IAHR and IHR, Valencia, Spain, 22–25 April 2003, pp. 773–780.
[28] W. Zielke, Frequency-dependent friction in transient pipe flow, *Journal of Basic Engineering* 90 (1968) 109–115.
[29] A.E. Vardy, J.M.B. Brown, Transient, turbulent, smooth pipe friction, *Journal of Hydraulic Research* 33 (4) (1995) 435–456.